
Research Paper

The Effect of Film Thickness on Thermal Aerosol Generation

Dan J. Myers,^{1,3} Ryan D. Timmons,¹ Amy T. Lu,¹ Ron L. Hale,¹ Dennis W. Solas,¹
Pravin Soni,¹ and Josh D. Rabinowitz²

Received June 22, 2006; accepted August 22, 2006; published online December 19, 2006

Purpose. Rapid heating of thin films of pharmaceutical compounds can vaporize the molecules, which leads to formation of aerosol particles of optimal size for pulmonary drug delivery. The aim of this work was to assess the effect of coated film thickness on the purity of a thermally generated (condensation) drug aerosol.

Materials and Methods. Pharmaceuticals in their free base form were spray-coated onto stainless steel foils and subsequently heated and vaporized in airflow via a rapid resistive heating of the foil. Aerosol particles were collected on filters, extracted, and analyzed using reverse phase HPLC to assess the amount of degradation induced during the vaporization process.

Results. Condensation aerosols of five pharmaceuticals were formed from a wide range of film coating thicknesses. All five showed a roughly linear trend of increasing aerosol purity with decreasing film thickness, although with quite different slopes. These findings are consistent with a model based on general vaporization and degradation kinetics. Small non-uniformities in the film do not significantly alter aerosol purity.

Conclusions. Rapid vaporization of pharmaceuticals coated as thin films on substrates is an efficient way of generating drug aerosols. By controlling the film thickness, the amount of aerosol decomposition can be minimized to produce high purity aerosols.

KEY WORDS: aerosol; condensation; degradation; thermal; thickness.

INTRODUCTION

Equilibrium transition of condensed phase organic compounds into the gas phase is well understood, characterized by the vapor pressure curve. The vapor pressure is an exponential function of temperature; hence a simple increase of the temperature will lead to a greater fraction of the compound in the gas phase. For low vapor pressure compounds, high temperatures are typically required for full conversion to the gas phase at atmospheric pressure within a reasonable period of time. Unfortunately, simple exposure of organic compounds to high temperatures leads to unwanted thermal degradation. A well known example of this is the heating and burning of tobacco during cigarette smoking: while nicotine is vaporized and subsequently available for the user, there is significant degradation at the high temperatures in the cigarette, which results in toxic "tars" that the user simultaneously inhales. Recently, we have reported that the thermal vaporization of many organic compounds can be kinetically controlled to decrease decomposition products and yield

highly pure vapors (1). These vapors condense in air to form aerosols. The particle size of the aerosol is controlled by varying the airflow over the vaporizing compound such that the median particle size falls between about 1 and 3 μm . We call this process thermal aerosol generation.

One area which could utilize aerosol formation of organic compounds is drug delivery. Deep lung inhalation of pharmaceuticals has key advantages, including the convenience of inhaling, the large absorptive surface area (>100 m^2) (2) of the alveoli, and the thinness and permeability of the barrier separating the alveolar airspace from the pulmonary capillary bed, which allows the direct passage of absorbed drug from the pulmonary circulation to the arterial circulation. This latter point means that the drug is not subjected to first-pass hepatic metabolism. These factors enable inhaled drug to reach the systemic circulation and brain in less than a minute, if the particles are of appropriate size to reach and deposit in alveoli (approximately 1–3 μm diameter is considered ideal) (3), the particles dissolve rapidly, and the drug readily crosses from the alveoli to the bloodstream (4). As thermally generated aerosols can be controlled to meet these criteria, they are ideal for inhalation drug delivery. Rabinowitz *et al.* (1) demonstrated this rapid onset concept of thermally generated drug aerosols in a dog model. The popular migraine drug rizatriptan (Maxalt[®]) was administered by oral and subcutaneous routes and by inhalation of thermally generated aerosol. Inhalation produced the fastest pharmacokinetic and pharmacodynamic effects. Recently this work was expanded

¹Alexza Pharmaceuticals, Inc., 1020 East Meadow Circle, Palo Alto, California 94303, USA.

²Present address: Department of Chemistry and Lewis-Sigler Institute for Integrative Genomics, Princeton University, Princeton, New Jersey, USA.

³To whom correspondence should be addressed. (e-mail: dmyers@alexza.com)

to demonstrate rapid pharmacokinetics of thermal aerosols of the anti-emetic drug prochlorperazine (Compazine[®]) in human subjects (5). Rapid pharmacokinetics, essentially equivalent to an intravenous bolus, were achieved.

The major challenge in thermal aerosol generation is to produce pharmaceutically relevant quantities of drug aerosols without copious amounts of degradation products or other unwanted impurities. Cigarette smoking is clearly effective for nicotine delivery but generates hundreds of known toxic entities (6–8). We have found that one of the most important factors in limiting degradation of the thermally generated aerosol is the original drug coating film thickness. Generally, other parameters, such as substrate effects and airflow rate, are of lesser importance compared to the film thickness, with some interesting exceptions, and will be discussed in future publications.

MATERIALS AND METHODS

Chemicals and Reagents

Midazolam (Versed[®]), nalbuphine hydrochloride dihydrate (Nubain[®]), atropine, and oxybutynin chloride (Ditropan[®]) were obtained from Sigma. Nalbuphine hydrochloride dihydrate and oxybutynin chloride were converted into their free base forms by suspending in DI water, adding excess saturated sodium bicarbonate, and extracting with dichloromethane. Vardenafil free base was prepared from its hydrochloride salt (Levitra[®]) according to published procedures (9). Table I shows the structures of the five compounds, along with their molecular weights and melting points.

As vaporization substrates, we used 302/304 stainless steel foils, 0.125 mm thick by 12.5 mm wide by 63.5 mm long (Brown Metals Company, Cucamonga, CA). Foils were cleaned by sonicating in 6.5% Ridoline 298 (Henkel Surface Technologies, Madison Heights, MI) aqueous solution at 60°C for 5 to 10 min followed by thorough rinsing with DI water and acetone prior to use.

Drug Coating

Drug coating onto the stainless steel substrates was done by a precision spray process. The drug solutions were sprayed with an ultrasonic nozzle (60 kHz, Sono-Tek Corporation, Milton, NY) that was fed by a computer-controlled syringe pump (Pump 22, Harvard Apparatus, Holliston, MA). Typical spray rates were 0.3–6 $\mu\text{L/s}$. The substrates were held on a computer-controlled x - y - z table (IAI America, Torrance, CA), approximately 7 cm below the tip of the nozzle. Patterns of 20 by 12.5 mm were created on the substrate by continuous, steady movement of the x - y - z table. Films of different thicknesses were created by varying the rate of the syringe pump. To create films of very high uniformity, we used a coating mask and increased the distance from the ultrasonic nozzle to the substrate, so that the sprayed solution fanned out over a greater area. The coating mask, a thin aluminum plate containing a 20-mm wide rectangular slot that defined the coating pattern, rested a few millimeters above the substrate surface. The mask minimized film deposition outside of the intended pattern, thereby providing a highly uniform thickness over the coated area.

For linearly sloping films, the substrate area exposed to the sprayed drug solution was increased in four steps. For the

first pass, all but 4 mm of the mask opening was covered and the standard x - y - z table program was run. Next, the coating mask was opened to 8 mm wide and the coating program was run again at the same flow rate. This was repeated two more times, with openings of 12 and 16 mm. The flow rate was kept the same for all four coating runs, but was modified from the uniform case so that the average coating thickness across the entire substrate was equivalent to that of the homogeneous coating pattern.

For sinusoidally oscillating films, a different coating mask was used. Instead of having one 20-mm wide opening over the substrate (as used for the uniform coating), this coating mask had three 4-mm wide slits with 4 mm of spacing between them. Again, the standard x - y - z table program was run, and the flow rate was modified so that the sinusoidal film had the same average thickness as the uniform film.

Rather than a direct measurement of the coating thickness, we typically use coating density (mass per surface area) as the thickness metric. However, an actual thickness value is more intuitive in the discussion that follows, and is calculated by

$$\lambda = \frac{\text{mass}}{\rho * SA}, \quad (1)$$

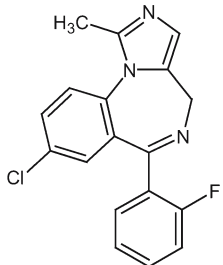
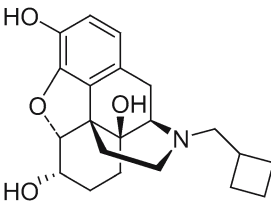
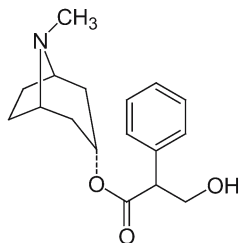
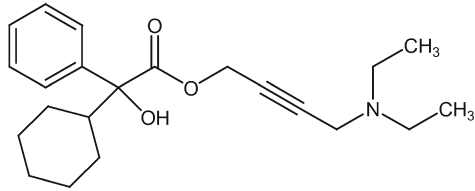
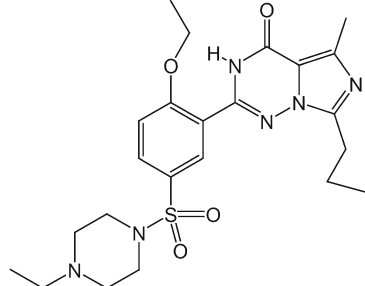
where λ is the thickness, SA is the surface area of the film coating, and ρ is the density of the coating. The density is generally assumed to be 1.0 g/cm^3 , unless a literature value is known. Therefore, 1 mg deposited over an area of 5 cm^2 results in a coating thickness of 2 μm . The coating thickness is most easily varied by altering the coating solution concentration or the syringe pump rate. For each of the specially patterned films (the highly uniform, the sinusoidally oscillating, and the linearly sloping films), we mapped the thickness profile by spray coating onto thin (1 mm wide) stainless steel strips, 20 of which were aligned side-by-side together to form an area equivalent to that coated on the vaporization substrates. After coating, the strips were individually extracted and quantitatively assayed via HPLC. Since the coated surface area of each strip was known, the drug thickness over each mm strip was estimated with the equation given above.

Thermal Aerosol Generation

The drug coated foils were placed inside a custom airway, which consisted of a machined plastic (Delrin[®]) block with a 3.2 cm^2 cross-sectional area for airflow. Brass electrodes attached to the Delrin[®] were used to clamp the foil in place and provide electrical connections. For most experiments, a 1 Farad capacitor was used as the energy source, typically charged to 11–14 V, depending on the required temperature for the foil. A high current relay (model type 120-105711, White-Rodgers/RBM) was used to connect the circuit and discharge the capacitor across the coated stainless steel foil. Figure 1 shows the heating profiles of the foils with 1 m/s airflow, as measured by an infrared camera (Thermacam SC 3000, FLIR Systems). The peak temperature is reached in ~ 100 ms.

For all purity experiments detailed here, the airflow rate was set to 15–20 L/min (air velocity of ~ 1 m/s). The airflow was established with a house vacuum system and consisted of non-filtered room air. The complete heating and vaporization

Table I. Compounds Used in Vaporization Experiments

Compound	Structure	Molecular weight	Melting Point (°C)
midazolam		325.8	158-160 ¹
nalbuphine		357.4	231 ¹
atropine		289.4	114-116 ¹
oxybutynin		357.5	N/A (viscous oil)
varденаafil		488.6	185-186 ²

¹From Merck Index, 13th edition.

²Measured on standard melting point apparatus (Thomas Hoover capillary melting point apparatus).

event occurs in a few hundred milliseconds. All of the compound is vaporized from the stainless steel surface. This is confirmed by extraction and quantitative HPLC analysis of the substrates after the vaporization process. Virtually no drug deposits on the inside surface of the airway.

Aerosol Collection and Purity Analysis

Drug aerosol was captured in 2 μm Teflon[®] filters (Zefluor[®]), which were subsequently extracted in HPLC

grade acetonitrile or, in the case of atropine, methanol. To confirm complete collection of the vaporized drug, experiments were occasionally also conducted with multiple filters and/or -70°C cold traps in series. Extraction of these filters and traps revealed no detectable drug or decomposition products passing through the first Teflon[®] filter. Extraction of the Teflon[®] filter with additional solvents, including dichloromethane and water, revealed no additional decomposition products not extracted with acetonitrile or methanol. The filter extracts were analyzed by high performance liquid

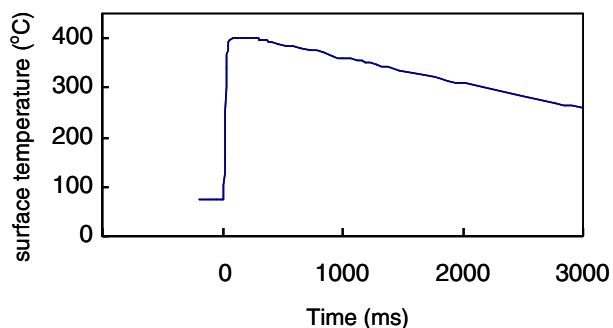


Fig. 1. Temperature of stainless steel foil during capacitive discharge (charged to 13.5 V). Temperature is measured with an infrared camera (Thermacam SC 3000, FLIR Systems), using an emissivity value of 0.17 for the stainless steel. Peak temperature is reached in ~ 100 ms.

chromatography (HPLC) using a C-18 reverse phase column (4.6 mm ID \times 150 mm length, 5 μ m packing, “Capcell Pak UG120,” Shiseido Fine Chemicals, Tokyo, Japan) and a mobile phase of water/0.1% trifluoroacetic acid (A) and acetonitrile/0.1% trifluoroacetic acid (B). The gradient went from A:B 95%:5% to 0%:100% with a flow rate of 1 mL/min and detection from 200 to 400 nm using a photodiode array detector. The purity is measured as the percentage of the drug peak area relative to the cumulative area of all peaks in the chromatogram at 225 nm. Confirmatory purity evaluations were additionally performed by inspection of the full 200–400 nm wavelength range. This qualitative analysis did not reveal major impurities other than those resolved at 225 nm.

Aerosol Particle Sizing

Midazolam was coated at three different thicknesses (~ 2.7 , 6.1, and 11.7 μ m), keeping the total amount coated constant by altering the surface area of drug deposition. Using the thermal aerosol generator described above, aerosols were formed under a 30 L/min airflow and captured in a Next Generation Impactor (MSP Corporation) fitted with an induction port. Each stage of the impactor was extracted with acetonitrile and analyzed by an isocratic HPLC method (50:50 acetonitrile:water). From the quantitative data, the mass median aerodynamic diameter was calculated.

RESULTS AND DISCUSSION

Effect of Film Thickness

In a previous work (1) we illustrated the effects of vaporizing compounds, specifically the drugs sildenafil (Viagra[®]) and fentanyl, in a bulk, powder form inside of a furnace tube oven. Extensive degradation of the collected aerosol was found, significantly worse than the aerosol evolved from vaporization of thin films of the two compounds. The purpose of the current work was to explore the role of coating thickness in greater detail.

Using the apparatus described above in the “Materials and Methods” section, we examined vaporization/degradation of some common pharmaceutical compounds: midazolam, nalbuphine, atropine, vardenafil, and oxybutynin. Figure 2 shows the

aerosol purity for each compound over a wide range of coating thicknesses. Each point is the average of multiple data points, with representative error bars of one standard deviation shown for atropine, which are roughly the size of the data icons.

Another fundamentally important parameter of pharmaceutical aerosols is particle size, which determines the location of deposition in the respiratory tract. The effect of drug coating thickness on particle size was found to be relatively minor. For example, midazolam coatings of 2.7, 6.1, and 11.7 μ m yielded very nearly the same particle size (Table II). Theoretically, the particle size is determined by the concentration of particles in the air. Thus airflow rate should be a major factor in establishing particle size, which agrees with our experimental findings (1).

Derivation of Film Thickness–Aerosol Purity Trend

As observed in Fig. 2, the extent to which a change in film thickness affects aerosol purity is dependent on the particular compound. Some compounds vaporize with little degradation over a broad thickness range (e.g., midazolam) while other compounds (e.g., vardenafil) show greater sensitivity to the coated film thickness. Regardless, in most cases, the purity of the aerosol follows a roughly linear trend with the thickness. The source of the near-linearity can be derived from analysis of fundamental kinetic rate laws. Let us start by assuming that a uniform thin coating of thickness λ is vaporized to completion at a fixed temperature. λ has units of length (cm). Since evaporation is a zeroth order process (10), the thin coating will undergo a constant net vaporization rate per unit surface area, V_{net} (units of milligram per second per square centimeter). Thus, the time, in seconds, required for complete vaporization of the coating is

$$t_c = \rho\lambda/V_{\text{net}} \quad (2)$$

where ρ is the density of the film (units of mg per cubic cm) and will be assumed to be unity for the sake of convenience. Define A_0 as the amount of pure compound at time 0 and $A(t)$ as the amount of compound still intact (undegraded) at

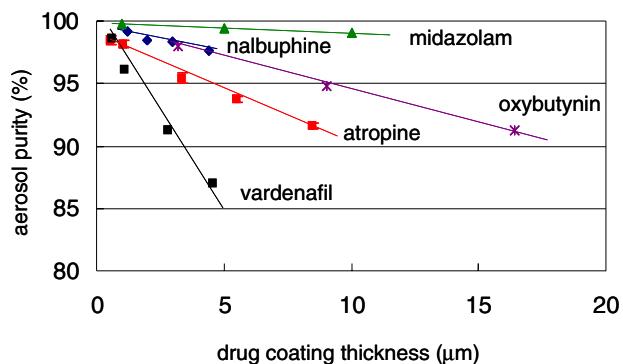


Fig. 2. Effect of drug film coating thickness on purity of thermally generated aerosol. Each point corresponds to an average of three data points, with the exception of vardenafil (average of two data points). One standard deviation error bars are roughly the size of the icons, as shown for atropine, and are otherwise omitted for clarity. The aerosol purities for all five drugs show a linear dependence on the film thickness, but with substantially different slopes.

Table II. Aerosol Particle Size (Mass Median Aerodynamic Diameter, MMAD) Resulting From Vaporization of Midazolam Films with Different Thicknesses

Film Thickness (μm)	MMAD (μm)
2.7	2.1 \pm 0.1
6.1	2.0 \pm 0.1
11.7	1.8 \pm 0.1

In each case, the coated dose amount was about the same (0.7 mg). The particle size numbers are averages of three data points along with one standard deviation.

time t . Likewise, let $D(t)$ represent the amount of degradants formed up to time t . Thus the purity of the vaporized compound is given by the equation

$$\begin{aligned} \text{purity} &= \frac{A(t_c)}{A(t_c) + D(t_c)} = \frac{A(t_c)}{A_o} = \frac{A_o - D(t_c)}{A_o} \\ &= 1 - \frac{D(t_c)}{A_o} \end{aligned} \quad (3)$$

Now consider some typical rate laws for possible decomposition reactions of A:

(1) Zeroth order (such as some surface-catalyzed decomposition reactions (11,12)). In the zeroth order case, the degradation is simply a linear function of time

$$D(t_c) = k_{\text{deg}} t_c = k_{\text{deg}} \lambda / V_{\text{net}} \quad (4)$$

and therefore

$$\text{purity} = 1 - \frac{k_{\text{deg}}}{A_o V_{\text{net}}} \lambda \quad (5)$$

where k_{deg} is the zeroth order rate constant. Thus the purity of the vaporized compound is linearly proportional to the original coating thickness.

(2) First order (such as many simple bond breaking (homolysis) mechanisms (12–14)). In first order processes, the degradant amount is given by

$$D = A_o (1 - e^{-k_{\text{deg}} t_c}) \quad (6)$$

with k_{deg} as the first order rate constant. Now the thermal aerosol purity is

$$\text{purity} = 1 - \frac{D}{A_o} = e^{-k_{\text{deg}} t_c} \stackrel{k_{\text{deg}} \text{small}}{\approx} 1 - k_{\text{deg}} t_c = 1 - \frac{k_{\text{deg}}}{V_{\text{net}}} \lambda \quad (7)$$

where we have used the limit of small degradation to expand the exponential term. Once again, the aerosol purity is a linear function of the coating thickness.

(3) Second order (such as many bimolecular and polymerization reactions (12,15)). In second order processes, the degradant amount is given by

$$D = A_o \left(1 - \frac{1}{1 + A_o k_{\text{deg}} t_c} \right) = \frac{A_o^2 k_{\text{deg}} t_c}{1 + A_o k_{\text{deg}} t_c} \quad (8)$$

with k_{deg} as the second order rate constant. In the limit of small degradation, the thermal aerosol purity is

$$\begin{aligned} \text{purity} &= 1 - \frac{D}{A_o} = \frac{1}{1 + A_o k_{\text{deg}} t_c} \\ &= \frac{1 - A_o k_{\text{deg}} t_c}{1 - A_o^2 k_{\text{deg}}^2 t_c^2} \stackrel{k_{\text{deg}} \text{small}}{\approx} 1 - A_o k_{\text{deg}} t_c \\ &= 1 - \frac{A_o k_{\text{deg}}}{V_{\text{net}}} \lambda, \end{aligned} \quad (9)$$

and the linear dependence comes out once more.

These cases represent simple approximations of more complicated decomposition processes which may occur with some drug compounds, particularly when multiple degradation products are formed. However, the arguments above capture the essence behind the roughly linear dependence observed in Fig. 2.

EFFECT OF FILM NON-UNIFORMITY

The discussion above assumed uniform chemical films. However, uniformly thick films can be challenging to construct on rough (non-silicon wafer) surfaces. Given the important effect of film thickness on aerosol purity shown above, one might think that film nonuniformity would have a significant effect on thermal aerosol generation. To examine the effect of nonuniformity, it is useful to consider two practical instances of variable film thickness.

Case of Linearly Sloping Drug Film

Assume that decomposition at any (x,y) point in the film depends linearly on the film thickness at that point

$$D(x,y) = \beta C(x,y) \quad (10)$$

where β is a proportionality constant, $D(x,y)$ is the fractional decomposition at point (x,y) , and $C(x,y)$ is the thickness at that point. The fractional decomposition over the entire surface of the film is thus

$$D = \int_x \int_y \frac{C(x,y)}{\bar{C}} D(x,y) dx dy \quad (11)$$

where \bar{C} is the average film coating thickness. The factor $C(x,y)/\bar{C}$ is a weighting factor that accounts for the fact that there is more of the chemical in the thicker regions. Now for the specific case of a linearly sloping plane, the film thickness can be defined by

$$C(x,y) = b + 2cx + 2dy \quad (12)$$

where b , c , and d are positive constants. For ease of calculation, let's normalize the plane coordinates, so that x and y span from 0 to 1. Thus

$$\bar{C} = \int_0^1 \int_0^1 C(x,y) dx dy = b + c + d \quad (13)$$

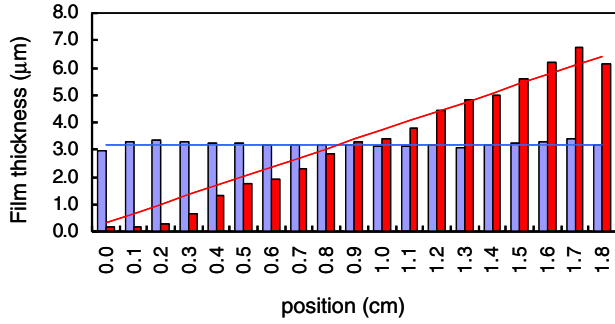


Fig. 3. Thickness variations for a uniformly coated film and a linearly sloping film of atropine. Both films were produced by spray coating and have the same average thickness. The linearly sloping film represents such situations as spraying onto a tilted surface or dip coating.

and so

$$D = \beta \int_0^1 \int_0^1 \frac{(b + 2cx + 2dy)^2}{b + c + d} dx dy$$

$$= \frac{\beta}{b + c + d} (b^2 + \frac{4}{3}c^2 + \frac{4}{3}d^2 + 2bc + 2bd + 2cd) \quad (14)$$

Note that if the film was completely uniform, then

$$D_{\text{even}} = \beta \bar{C} = \beta(b + c + d), \quad (15)$$

and the ratio of degradation between the actual sloping film and the ideal uniform film is

$$D/D_{\text{even}} = \frac{b^2 + \frac{4}{3}c^2 + \frac{4}{3}d^2 + 2bc + 2bd + 2cd}{(b + c + d)^2}$$

$$= \frac{(b + c + d)^2 + (\frac{1}{3}c^2 + \frac{1}{3}d^2)}{(b + c + d)^2}$$

$$= 1 + \frac{c^2 + d^2}{3(b + c + d)^2} \quad (16)$$

$$< 1 + \frac{c^2 + d^2}{3(c + d)^2}$$

$$< 1 + \frac{1}{3}$$

Thus the worst case scenario shows only one-third more degradation than the perfectly uniform film. In reality, surface irregularities of the thin film would be leveled out somewhat as the intermolecular forces are overcome during heating. However, this leveling likely would be limited to fairly small areas given the short times before evaporation.

This example is of particular relevance because it closely represents the theoretical thickness distribution of typical films made through the dip coating process (16), as shown in Fig. 3. Figure 3 also shows the distribution from a more carefully controlled spray coating process where the film is very uniform. The aerosol impurities resulting from the vaporization of these two drug films are captured in Table III. Note that the uneven film produces about 28% more degradation than the uniform film, in good agreement with the theoretical prediction above. This is an extreme case, where the large thickness difference between the two ends is easily visible to the naked eye.

Table III. Aerosol Impurity Resulting from Vaporization of Atropine Films with Average Thickness of about 3.2 Microns

Film Type	Aerosol Impurity (%)
Uniform	4.6±0.4
Linearly sloping	5.9±0.3
Sinusoidally oscillating	5.5±0.1

The impurity numbers are averages of five data points along with one standard deviation.

Case of Sinusoidally Varying Film

Let's now consider the case of a film oscillating about some average thickness in one axis (say the x -axis). The film pattern is given by

$$C(x, y) = \bar{C} + c^* \sin(2\pi dx) \quad (17)$$

with $c < \bar{C}$ (so C does not become negative) and d a positive integer, to simplify the math. Therefore the relative amount of decomposition compared to the even film is

$$D/D_{\text{even}} = \frac{\int_0^1 [\bar{C} + c^* \sin(2\pi dx)]^2 dx}{\bar{C}^2}$$

$$= \frac{\bar{C}^2 + \frac{1}{2}c^2}{\bar{C}^2} \quad (18)$$

$$< 1 + \frac{1}{2}$$

The worst case scenario for the oscillating film has only 50% more degradation than the perfectly uniform film. In an actual vaporization event, surface unevenness would likely get partially smoothed out, as in the sloping film, during heating of the thin film.

The sinusoidally oscillating case is representative of a spray coating process where the spray head is held very close to the surface and the substrate (or nozzle) travels in a serpentine style pattern during the coating event. In this case, the coated area directly underneath the nozzle will be thicker, while the troughs between consecutive rows will be thinner. By manipulating the coating method, we created an idealized sinusoidal pattern, as shown in Fig. 4 (along with the uniform

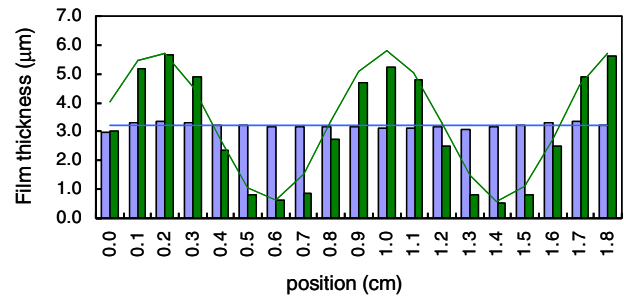


Fig. 4. Thickness variations for a uniformly coated film and a sinusoidally oscillating film of atropine. Both films were produced by spray coating and have the same average thickness. The oscillating film represents cases where the spray pattern does not fan out enough to overlap consecutive passes.

film pattern). The thickness is well fit with the equation $\lambda = 3.2 + 2.6^* \sin [2\pi(x + 0.12)]$.

Table III shows aerosol purity data stemming from vaporization of the oscillating film, again in comparison to the uniform film. Note that the oscillating film yields about 20% more degradation, less than the theoretical maximum. As suggested above, local variations in film thickness are probably evened out to some degree prior to vaporization as a result of heating of the film.

CONCLUSION

Thermal aerosol generation provides a means for making aerosols of a large number of organic compounds of relatively low ambient vapor pressure. While most such compounds are generally thought to be thermally labile, the use of thin coatings, which increases the rate of vaporization relative to the rate of decomposition, results in highly pure aerosols. As discussed in more detail in a previous paper (1), control of the airflow over a vaporizing compound primarily determines the resulting particle size, independent of the exact nature of the chemical. Important contributions of the present manuscript include identification of the quantitative, roughly linear relationship between coating thickness and aerosol purity, and demonstration that the thermal aerosol generation process is robust to small variations in the coating uniformity.

The technique of thermal aerosol generation has potential applications in areas where relatively uniformly sized, highly pure particles in the micron size range are desirable. Of these, the most immediate application is inhalation drug delivery, where aerosol particles of the proper size have the potential to improve the efficacy of some medications administered by inhalation, including ones targeting the pulmonary tract (by depositing them directly at their site of action) and those acting systemically (by increasing their bioavailability and/or accelerating their time of onset). In this paper we have demonstrated highly pure aerosols of several pharmaceutical compounds, including atropine, midazolam, vardenafil, oxybutynin, and nalbuphine. This set of compounds encompass a wide variety of pharmaceutical applications, including nerve gas poisoning, seizures, erectile dysfunction, incontinence, and pain relief. A fast-acting medical product could provide significant medical benefits for any of these conditions. In clinical testing, products utilizing this technology have demonstrated safe and reproducible systemic drug delivery as well as efficacy in a patient population (5).

ACKNOWLEDGMENTS

We acknowledge Dan Mufson and Edwin Kamemoto for their suggestions in preparation of this manuscript. We also acknowledge the assistance of Kathleen Simis in the design and preparation of materials for particle size experiments.

REFERENCES

1. J. D. Rabinowitz, M. Wensley, P. Lloyd, D. Myers, W. Shen, A. Lu, C. Hodges, R. Hale, D. Mufson, and A. Zaffaroni. Fast onset medications through thermally generated aerosols. *J. Pharmacol. Exp. Ther.* **309**:769–775 (2004).
2. W. M. Thurlbeck. The internal surface area of nonemphysematous lungs. *Am. Rev. Respir. Dis.* **95**:765–773 (1967).
3. J. Heyder. Particle transport onto human airway surfaces. *Eur. J. Respir. Dis. Suppl.* **199**:29–50 (1982).
4. C. Ehrhardt, J. Fiegel, S. Fuchs, R. Abu-Dahab, U. F. Schaefer, J. Hanes, and C. M. Lehr. Drug absorption by the respiratory mucosa: cell culture models and particulate drug carriers. *J. Aerosol Med.* **15**:131–139 (2002).
5. J. D. Rabinowitz, P. M. Lloyd, P. Munzar, D. J. Myers, S. Cross, R. Damani, R. Quintana, D. A. Spyker, P. Soni, and J. V. Cassella. Ultra-fast absorption of amorphous pure drug aerosols via deep lung inhalation. *J. Pharm. Sci.* **95**:2438–2451 (2006).
6. R. L. Stedman. The chemical composition of tobacco and tobacco smoke. *Chem Rev.* **68**:153–207 (1968).
7. I. Schmeltz and D. Hoffmann. Nitrogen-containing compounds in tobacco and tobacco smoke. *Chem Rev.* **77**:295–311 (1977).
8. A. S. Freeman and B. R. Martin. Quantification of phenacyclidine in mainstream smoke and identification of phenylcyclohex-1-ene as pyrolysis product. *J. Pharm. Sci.* **70**:1002–1004 (1981).
9. U. Niewohner, M. Es-Sayed, H. Haning, T. Schenke, K. Schlemmer, J. Keldenich, E. Bischoff, E. Perzborn, K. Dembowski, P. Serno, and M. Nowakowski. 2-phenyl substituted imidazotriazinones as phosphodiesterase inhibitors. International Patent WO 99/24433, May 20, 1999.
10. P. W. Atkins. *Physical Chemistry*, Freeman, New York, 1990.
11. G. Schwab and N. Theophilides. The absolute decomposition velocity of vapors. *J. Phys. Chem.* **50**:427–440 (1946).
12. K. J. Laidler. *Chemical Kinetics*, Harper & Row, New York, 1987.
13. K. A. Holbrook, M. J. Pilling, and S. H. Robertson. *Unimolecular Reactions*. Wiley, Chichester, 1996.
14. C.H. Bamford and C.F. Tipper (eds.). *Comprehensive Chemical Kinetics: Decomposition and Isomerization of Organic Compounds*, vol. 5, Elsevier, Amsterdam/New York, 1972.
15. M. S. El-Shall, A. Bahta, H. Rabeony, and H. Reiss. Homogeneous gas phase thermal polymerization of styrene. *J. Chem. Phys.* **87**:1329–1345 (1987).
16. L. E. Scriven. Physics and applications of dip coating and spin coating. *Mat Res Soc Symp Proc.* **121**:717–729 (1988).